

Original Research

# Weathering of Clay-Pyrite of Coal-Bearing Formation in the Endemic Fluorosis Area of Southwest China

Hong Xiuping<sup>1</sup>, Yang Kang<sup>2\*</sup>, Liang Handong<sup>3</sup>, Wang Xin<sup>1</sup>

<sup>1</sup>College of Life Science, Huaibei Normal University, Huaibei, Anhui, China, 235000, China

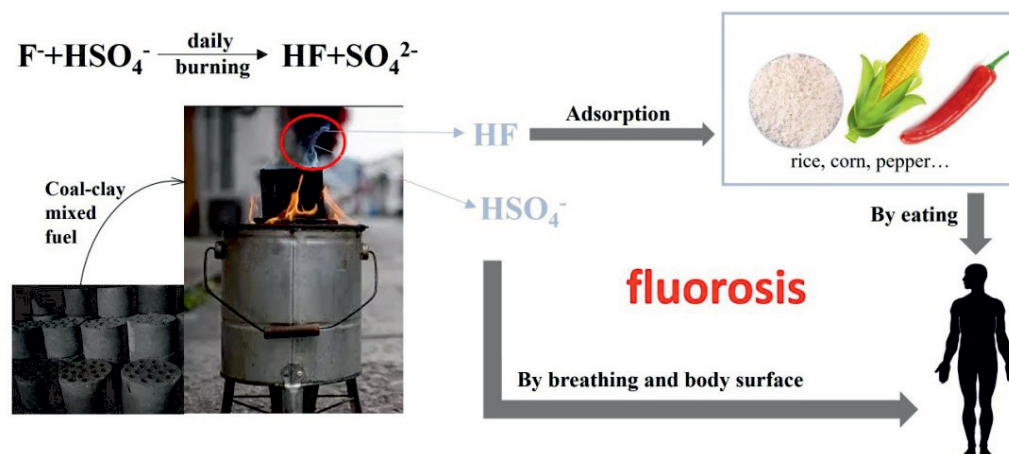
<sup>2</sup>School of Chemical & Environmental Engineering, CUMTB, Beijing 100083, China

<sup>3</sup>State Key Laboratory of Coal Resources and Safe Mining, CUMTB, Beijing 100083, China

Received: 29 August 2022

Accepted: 21 October 2022

## Abstract



It is common practice to use clay for coal-burning in fluorosis areas on the border of Yunnan, Guizhou, where coal-bearing strata is widely outcropped, and clay for coal-burning is usually considered to be collected from efflorescent clay in coal-bearing strata by some scholars. However, the relevant chemical properties of the clay, the mechanism that causes the fluorosis are not clear and the chemical forms of fluorine species present during transfer from the clay to the human body remain unclear. In this study, approximately 71 samples of efflorescent clay of coal-bearing strata were collected from seven counties in this area, and the results showed that those samples had a high-fluorine content with an average of  $751 \mu\text{g}\cdot\text{g}^{-1}$  ( $237\text{--}1,764 \mu\text{g}\cdot\text{g}^{-1}$ ,  $n = 71$ ). The clays were rich in acid with an average pH of 5.81 (2.39-8.25,  $n = 71$ ) and the acidic clays accounted for 52% of the total clay samples. The sulfate ( $SO_4^{2-}$ ) content

of the clay samples were also high and ranged from 295 to 13086  $\mu\text{g}\cdot\text{g}^{-1}$  (average 1851  $\mu\text{g}\cdot\text{g}^{-1}$ ,  $n = 71$ ). The pH value of the acidic efflorescent clay was positively correlated with  $-\lg C [\text{SO}_4^{2-}]$  ( $R = 0.75$ ), which indicated that the acid may exist in the form of acidic sulfate such as  $\text{KHSO}_4$  or  $\text{NaHSO}_4$ . Further research using time-of-flight secondary ion mass spectrometry (TOF-SIMS) found that the surface of the clay samples was rich in characteristic positive and negative ions such as  $\text{HSO}_4^-$ ,  $\text{SO}_4^-$ ,  $\text{FeSO}_4^+$ ,  $\text{FeO}^+$ , and  $\text{F}^-$ . This indicated that the clay samples contained pyrite and the pyrite in clay had been weathered and produced acid sulfate as a result of long-term natural exposure to coal strata. By heating the clay samples, hydrogen fluoride (HF) was released from the clay and it was verified quantitatively without exception, ranging from 28 to 302 ppb (average 105.67 ppb), which was significantly higher than the HF background concentration in the laboratory. The result provided direct evidence of HF release during the heating process. The possible reaction mechanism was that a chemical reaction between the acid ( $\text{HSO}_4^-$ ) and fluorine in the clay occurs, thereby producing HF, which is the chemical form of fluorine released from clay under relatively mild conditions. The unique chemical and physical properties of HF may provide new insights into the pathogenic mechanisms of coal-burning induced endemic fluorosis.

**Keywords:** fluorosis, clay-pyrite, acid sulfate, time-of-flight secondary ion mass spectrometry, Guizhou province

## Introduction

The once-endemic fluorosis in southwest China, especially in rural areas, was serious and persistent [1-5]. More than 16.1 million dental fluorosis patients and 1.8 million skeletal fluorosis patients were documented in China in 2008 and have been linked to coal-burning pollution [6, 7]. Heavy endemic fluorosis affects northeastern Yunnan, northwestern Guizhou, and southern Sichuan provinces, which contain villages covering large areas and accounting for 73% of all fluorosis villages in the coal-burning fluorosis areas of China. More than 70% of these fluorosis patients live in western Guizhou and eastern Yunnan provinces [8-11].

Pathological endemic fluorosis in southwestern China is thought to be correlated with the local household practice of burning domestic coal in an open stove, which releases fluorine into indoor air through combustion. This results in the contamination of stored food, such as chili peppers and corn, which leads to chronic fluorine poisoning of the body through continuous ingestion [7, 12-16]. Advances in the research and documentation of fluorine content data for coal in Guizhou and adjacent provinces have prompted interest in the use of clay binder in coal. Zhou and Fu [17], Zhou et al. [18] first discussed the role of clay binders and proposed that it is the main source of fluorosis in areas without high coal fluorine contents. Wu et al. [19], Dai et al. [20], Chen et al. [21], and Li et al. [22] further confirmed the role of the high fluorine content clay binder in coal-burning fluorosis, providing a theoretical basis for establishing fluorosis prevention and control measures. Nevertheless, it remains difficult to explain the process by which fluorine is released during combustion, which leads to long-term human exposure. This is because the fluorine in clay exists mainly in the form of fluorine compounds that are stable and have a high boiling point, such as calcium oxide and calcium fluorophosphates [23-26].

Using time-of-flight secondary ion mass spectrometry (TOF-SIMS) combined with on-site coal combustion tests, Liang et al [27] verified that naturally outcropping coal, commonly used by locals, was rich in sulfuric acid. This led to the proposition of a new perspective: during usage of coal-fired systems, sulfuric acid facilitates the release of fluorine in the form of hydrogen fluoride (HF), which then pollutes the environment. This theory has received widespread attention [28]. Our recent study on the sulfur-rich coal-bearing strata of the Late Permian Longtan Formation, which outcrops naturally in northwest China and is widespread in adjacent regions, found that the clay in the formation was generally rich in fluorine (F), acid ( $\text{H}^+$ ) and sulfate ( $\text{SO}_4^{2-}$ ) [29,30] and optical microscopy observations have confirmed that typical sulfide pyrite ( $\text{FeS}_2$ ) is commonly found in the efflorescent clays [24, 31]. In fact, the clay for coal-burning in this area was the efflorescent clay at the bottom of Longtan Formation. Although the general mechanism of coal-burning fluorosis is understood, the form of acid in clay is not clear and the chemical forms of fluorine species present during transfer from the clay to the human body still remain unclear.

Herein, we present preliminary statistics for the acidity and sulfate contents of clay samples in eight counties of the junction area of Yunnan, Guizhou, and Sichuan provinces. In this study heating experiments were performed to explore the possible mechanism of fluorine release from clay and to discuss whether the acid in the regolith can promote the release of fluorine in the clay. TOF-SIMS was used to confirm the presence of pyrite and acidity in the clay from coal-bearing strata. This study will help to further understand the role of clay for coal-burning in fluorosis and provide a scientific basis for the prevention and treatment of fluorosis.

## Materials and Methods

### Study Area

Cross-sectional and systematic clay samples were collected from 8 of the 21 counties in the coal production area. This area is situated at the junction of Yunnan, Guizhou, and Sichuan provinces, and in the transition zone of the Yunnan-Guizhou Plateau and Sichuan Basin in southwestern China, namely Weixin and Zhenxiong counties in eastern Yunnan province; Chishui, Hezhang, Dafang, and Xijiu counties in western Guizhou Province; and Guilin and Xuyong counties in southern Sichuan province (Fig. 1). These study sites, which are the heaviest fluorosis zones in China, are major coal mining regions and the main source of domestic coal in southwestern China [32, 33]. The Longtan Formation of the Late Permian is the main coal mining bed in this area, and the carbonate rock consists mainly of Cambrian and Triassic carbonates.

The study area is reportedly affected by a subtropical and warm plateau monsoon climate, with most of the area being characterized as karst mountainous with an undulating landscape. The area is heavily dissected by streams and rivers that are fed by seasonal rain. The climate varies with altitude and is cool and rainy with an annual temperature of 11-18°C and annual precipitation of 900-1,200 mm at high altitudes [34]. The annual duration of sunshine is less than 1,500 h.

### Sample Collection and Preparation

The sampling work was guided by county-level highways, and sampling interval was considered. In total, 69 clay samples were collected from the natural outcropping clay layer of the Longtan Formation coal mining regions in the study area. The locations of the sampling points are shown in Fig. 1. It is commonly

observed that the clay is used for coal-burning in fluorosis areas in southwestern China, where coal-bearing strata are widely outcropped, and clay for coal-burning is usually considered to be collected from efflorescent clay in coal-bearing strata [35]. All collected samples were loaded into poly sealed vinyl Ziplock bags. Samples were air-dried and sieved to a size of less than 150 mesh for chemical analysis.

### Analytical Methods

#### *Determination of Total Fluorine, Acidity, and Sulfate in Clay*

The total fluorine in the clay was determined using a combustion-hydrolysis fluoride ion-selective electrode method in accordance with the Chinese National Standards (GB4633-1997) [29]. A composite fluorine ion electrode (perfect ION mode) provided by Mettler Toledo (Switzerland) was coupled with an electrometer (Mettler Toledo) for analysis. Standard soil samples GBW07403 and GBW07406, provided by the National Standard Material Center, were used as quality controls.

The clay sample acidity test method was based on a previous study [30]. The electrometer was calibrated using three types of standard pH buffer solutions (at pH values of 4.01, 7.00, and 9.02; Mettler Toledo) prior to measurement. Before measurement, a sample of the original coal (20 g) was dissolved in water (50 mL), subjected to ultrasound for 1 h, left to stand for 6 h, filtered, and analyzed.

The sulfate content of the clay was determined using ion chromatography method [36]. Standard recovery test was used to control the quality, and the sample recovery was controlled in the range of 75%-135%. The standard deviation of parallel samples is less than 30%.

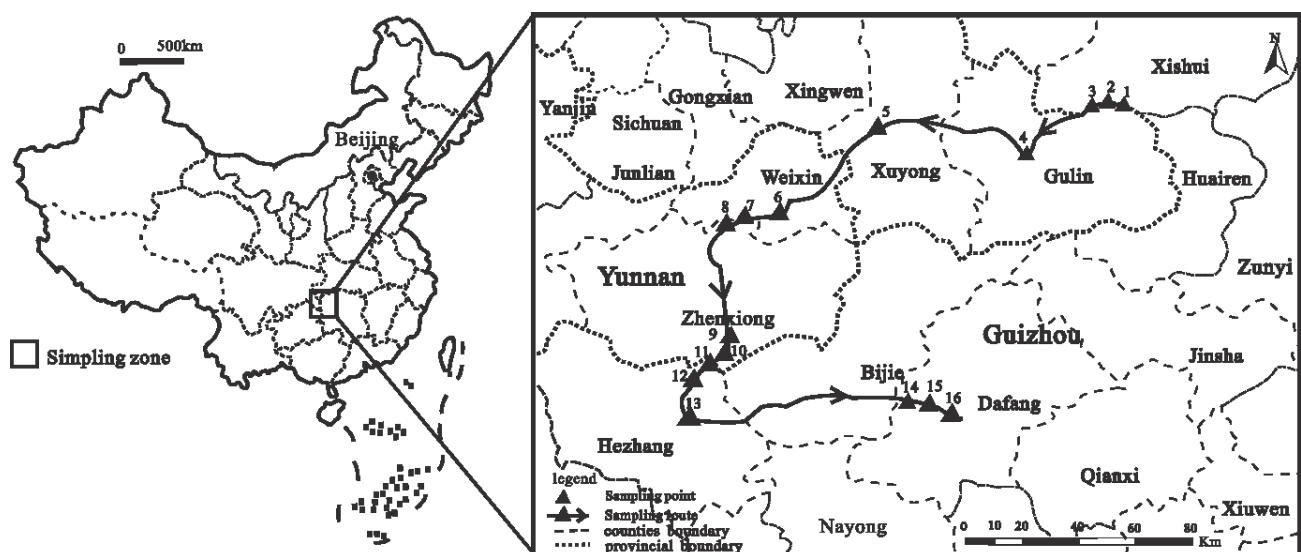


Fig. 1. Sampling locations.

## TOF-SIMS Analysis

After being subjected to curing with epoxy resin, cutting, grinding, and polishing, test samples in the form of 13 mm × 13 mm × 2 mm blocks were created. The fresh pyritic surface was observed under a microscope.

A TOF-SIMS instrument (TOF-SIMS.5-100, IONTOF, Germany) was used to obtain the mass spectra of the samples. The test samples were placed overnight in the vacuum chamber of the instrument. During the analysis, the quality of the main vacuum was maintained at above 1E-9 Pa. The preselected areas of the test samples were pre-sputtered using an O<sub>2</sub><sup>+</sup> gun to remove contaminants adsorbed on the surface. The source used for the analysis was Bi<sup>+</sup> with an acceleration voltage of 30 keV, a beam of 1 pA, and a scanning area of 400 × 400 μm.

First, the positive and negative ion mass spectra were collected in high mass resolution mode, with

the acquisition time of a single spectrum being 20 min. Next, the positive and negative ion mass spectra were separately collected in the burst mode, which concurrently considered high mass and spatial resolutions. Finally, the ion-imaging data were processed. Three microdomains (400 μm × 400 μm) on each of the 20 clay samples were analyzed, which produced 90 positive and negative mass spectrometric analyses. Various tests conducted on the different microzones of both the test and parallel samples produced consistent results.

## Results and Discussion

## Acidity and Sulfate in Clay

Table 1 shows that the mean pH of the clay samples was 5.98 (4.55-8.25) for eastern Yunnan, 5.40 (2.39-8.04)

Table 1. Chemical properties of clay samples.

Study area	Sample name	pH	SO <sub>4</sub> <sup>2-</sup> (μg/g)	T-F (μg/g)	W-F (μg/g)	HF (ppb)	Sample location	Location
Eastern Yunnan	MBT-1	4.85	962	689	8.32	104	Miaoba Village, Zhaxi Town, Weixin County, Yunnan Province	N:27°48'29.4" E:105°03'54.8" H:1088 m
	MBT-3	4.58	1033	641	6.43	125		
	GHT-1	8.25	366	869	10.49	42	Ganhe Village, Zhaxi Town, Weixin County, Yunnan Province	N:27°47'52" E:104°56'53.9" H:1297 m
	GHT-2	7.73	295	795	3.61	78		
	GHT-3	5.31	2968	809	9.21	118		
	GHT-4	5.66	679	457	3.02	105		
	GHT-5	5.54	784	790	4.21	126		
	GHT-6	5.08	2997	833	10.3	120		
	GHT-7	5.28	1313	802	9.64	113		
	GHT-8	7.81	345	598	4.13	76		
	GHT-9	6.35	447	850	11.2	89		
	GHT-10	8.19	551	653	2.92	34		
	GHT-11	6.03	1240	791	8.45	80		
	DHZT-1	7.32	1139	691	7.03	76	Daihaizi village, Zhenxiong County, Yuhe Town, Yunnan Province	N:27°46'35.9" E: 104°53'14.5" H:1041 m
	DHZT-2	7.27	1073	762	6.23	70		
	ZXT-1	4.82	1407	556	4.24	189	Zhenxiong County, Yunnan Province	N:27°21'01.8" E:104°52'13.5" H:1485 m
	ZXT-2	6.11	565	547	3.61	90		
	ZXT-3	5.98	934	522	1.51	88		
	ZDHT-1	4.55	1039	835	7.21	189	the edge of Zhenxiong county, Yunnan Province	N:27°24'29.2" E:104°52'53.4" H:1641 m
	ZDHT-2	5.2	982	755	9.58	110		
ZDHT-3	5.12	962	713	9.17	90			
ZDHT-4	5.28	813	691	6.23	112			
ZDHT-5	5.36	827	883	14.26	136			

Table 1. Continued.

Western Guizhou	XJT-1	7.59	1173	739	13.02	53	A coal wharf in Xijiu Town, Xishui County, Guizhou Province	N:28°09'59.3" E:106°07'59.4" H:1103 m
	XJT-2	7.7	1292	718	10.71	88		
	XJT-3	8.02	759	460	2.23	60		
	CST-2	8.04	696	380	2.78	53	Chishui River, Guizhou Province	N:28°09'04.5" E:106°03'54.1" H:853 m
	CST-3	3.67	5678	625	3.43	100		
	CST-4	2.8	7137	655	4.21	273		
	ZMXT-1	5.18	3505	909	16	78	Zhemuxue Village, Hezhang County, Guizhou	N:27°20'7.6" E:104°50'41.6" H:1631 m
	ZMXT-2	7.33	813	893	19.6	89		
	ZMXT-3	6.86	798	409	2.66	150		
	ZMXT-4	4.61	2188	760	9.21	202		
	ZMXT-5	4.77	6554	686	8.62	170		
	ZMXT-6	4.3	4819	586	1.81	135		
	ZMXT-7	7.18	528	448	1.47	90		
	ZZT-1	4.72	845	632	3.22	118	Zhezhuang Village, Hezhang County, Guizhou Province	N:27°17'53.0" E:104°47'31.7" H:1838 m
	ZZT-2	4.74	773	765	10.43	91		
	ZZT-3	5.09	998	548	3.99	98		
	HMT-1	5.53	876	775	12.94	101	Haima Village, Hezhang County, Guizhou Province	N:27°09'36.7" E:104°44'39.6" H:1473 m
	HMT-2	5.87	697	524	1.75	50		
	HMT-3	5.09	1093	466	1.83	89		
	HMT-4	5.29	1297	438	2.27	99		
	HMT-5	5.43	993	485	2.11	79		
	HMT-6	5.1	503	570	3.64	128		
	DF1T-1	6.17	1839	1317	12.22	28	Sampling point No. 1 along the highway in Dafang County, Guizhou Province	N:27°11'56.5" E:105°33'21.9" H:1449 m
	DF1T-2	6.51	1744	1578	18.9	60		
	DF1T-3	6.48	1875	1175	15.25	32		
	DF2T-1	2.45	12865	1764	19.42	165	Sampling point No. 2 along the highway in Dafang County, Guizhou Province	N:27°11'29.4" E:105°34'31.3" H:1550m
	DF2T-2	2.41	12737	1750	20.34	246		
DF2T-3	2.39	13086	1727	20.61	302			
DF2T-4	7.75	662	631	6.2	60			
DF3T-1	4.7	1478	875	9.61	133	Sampling point No. 3 along the highway in Dafang County, Guizhou Province	N:27°10'02.3" E:105°34'38.9" H:1584 m	
DF3T-2	4.53	1391	795	4.5	119			
DF3T-3	4.48	1585	573	3.28	150			
Northern Sichuan	ELZT-1	7.85	527	967	15.39	50	Erlang Town, Gulin County, Sichuan province	N:28°09'55.4" E:106°08'15.1" H:1148 m
	ELZT-2	7.79	613	940	12.2	51		
	GLT-1	7.98	675	362	1.91	43	Yudong River, West of Gulin County, Sichuan Province	N:27°59'00.8" E:105°48'16.1" H:632.6 m
	GLT-2	8.07	565	440	1.54	31		
	XYT-1	7.92	469	985	13.56	30	Tianshengqiao Village, Xuyong County, Sichuan Province	N:28°05'06.5" E:105°22'46" H:435 m
	XYT-2	4.54	1066	381	2.11	105		
	XYT-3	4.45	1060	237	1.81	150		
	XYT-4	6.47	540	691	7.34	110		
XYT-5	6.74	636	718	11.29	70			

Table 1. Continued.

Northern Sichuan	XYT-6	4.24	1400	767	8.97	189	Tianshengqiao Village, Xuyong County, Sichuan Province	N:28°05'06.5" E:105°22'46" H:435 m
	XYT-7	7.62	652	526	3.15	59		
	XYT-8	7.71	633	933	13.94	83		
	XYT-9	4.51	971	860	10.71	149		
	XYT-10	4.44	917	857	9.37	100		
	XYT-11	5.32	922	588	3.37	111		
	XYT-12	4.75	968	912	11.22	110		
	Min	2.39	295	237	1.47	28		
	Max	8.25	13086	1764	20.61	302		
	Average	5.81	1851.04	751.48	7.86	105.67		

for western Guizhou, and 6.45 (4.24-8.07) for northern Sichuan, with an overall mean pH for the three areas being 5.81 (2.39-8.25), which hints that the acidity of clays in northwestern Guizhou is generally stronger than that of clays in northeastern Yunnan and southern Sichuan. The pH values of the different samples varied widely, indicating that both acid clay and normal clay were present in all the three areas.

The pH of acid rain is less than 5.6 [37]. Accordingly, the clay samples in our study were classified as acidic clay ( $\text{pH} \leq 5.6$ ) or normal clay ( $\text{pH} > 5.6$ ). In the present study, 37 clays in the study area were classified as acidic clay, with pH values ranging from 2.39 to 5.54, with an average of 4.62; 34 clays were normal clays, with pH ranging from 5.66 to 8.25. The results clearly showed that strongly acidic clay was present throughout the study area, with the proportion of acidic clay equal to that of normal clay, which was in accordance with the clay in Qianxi County, Bijie City, Guizhou Province, as reported by He [4].

As shown in Table 1 and Fig. 2, the sulfate ( $\text{SO}_4^{2-}$ ) content of the clay in the study area was  $1,851 \mu\text{g}\cdot\text{g}^{-1}$  ( $295\text{-}13,086 \mu\text{g}\cdot\text{g}^{-1}$ ). The results showed that some

clays had abnormally high levels of sulfate, with notable variations between different samples. The sulfate content of clay from coal measure strata was the highest in western Guizhou, ranging from 503 to  $13,086 \mu\text{g}\cdot\text{g}^{-1}$ , with an average of  $2,871 \mu\text{g}\cdot\text{g}^{-1}$ , while the sulfate content ranged from 295 to  $2,998 \mu\text{g}\cdot\text{g}^{-1}$ , with an average of  $957 \mu\text{g}\cdot\text{g}^{-1}$  in eastern Yunnan clay, and from 469 to  $1,400 \mu\text{g}\cdot\text{g}^{-1}$ , with an average of  $788 \mu\text{g}\cdot\text{g}^{-1}$  in southern Sichuan coal. In acidic clay, the sulfate content varied from 421 to  $13,086 \mu\text{g}\cdot\text{g}^{-1}$ , with an average of  $2,406 \mu\text{g}\cdot\text{g}^{-1}$ , which was significantly higher than that of normal clay, which had an average of  $939 \mu\text{g}\cdot\text{g}^{-1}$  ( $295\text{-}4,819 \mu\text{g}\cdot\text{g}^{-1}$ ). The sulfate content of different samples varies greatly, which may be related to different degrees of exposure to the surface or can be affected by rainfall elution.

### Fluorine in Clay

Table 1 shows that the mean fluorine content of the clay samples was  $719 \mu\text{g}\cdot\text{g}^{-1}$  ( $457\text{-}883 \mu\text{g}\cdot\text{g}^{-1}$ ,  $n = 23$ ) in western Guizhou,  $802 \mu\text{g}\cdot\text{g}^{-1}$  ( $380\text{-}1,764 \mu\text{g}\cdot\text{g}^{-1}$ ,  $n = 32$ ) for eastern Yunnan,  $698 \mu\text{g}\cdot\text{g}^{-1}$  ( $237\text{-}985 \mu\text{g}\cdot\text{g}^{-1}$ ,  $n = 16$ ) for northern Sichuan, which indicates that there is little difference in the fluorine content among the different areas. The total average fluorine content in the three areas was  $751 \mu\text{g}\cdot\text{g}^{-1}$  ( $237\text{-}1,764 \mu\text{g}\cdot\text{g}^{-1}$ ,  $n = 71$ ), which was significantly higher than the background value of soil fluorine in China ( $478 \mu\text{g}\cdot\text{g}^{-1}$ ) and the world average ( $200 \mu\text{g}\cdot\text{g}^{-1}$ ), as reported by Hong [24] and Zheng [38]. However, the fluorine content in the study area tended to be consistent and approximated the average fluorine concentration ( $743 \mu\text{g}\cdot\text{g}^{-1}$ ) found in the Guizhou soil, as reported by Liu [7] and Pan [39]. Therefore, most of the clays in the study area were high-fluorine containing (more than  $200 \mu\text{g}\cdot\text{g}^{-1}$ ), which is in accordance with previous studies by Li [40] and Chen [21]. Studies have shown that high levels of fluorine in clay may be associated with high-fluorine montmorillonite in the mixed-layer minerals. Furthermore, water-soluble F was detected in all coal samples in the range  $1.47\text{-}20.61 \mu\text{g}\cdot\text{g}^{-1}$ ,

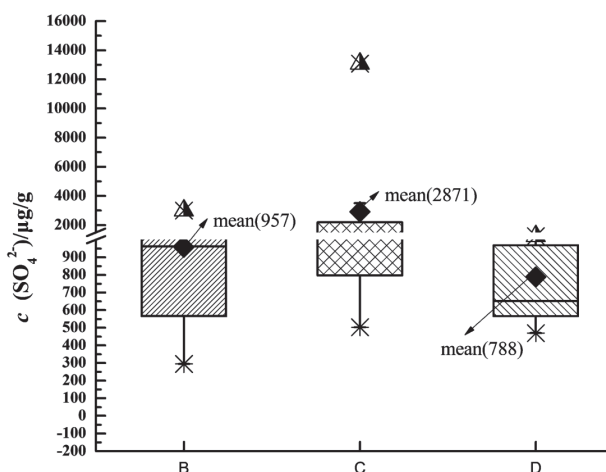


Fig. 2. Distribution of sulfate in efflorescent clay.

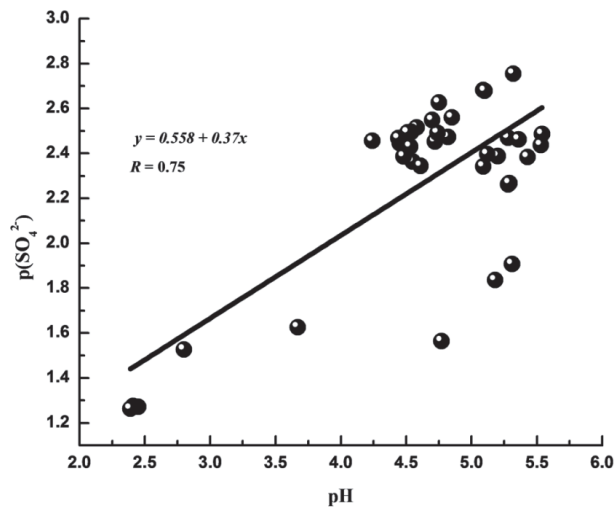


Fig. 3. Relationship between  $p(\text{SO}_4^{2-})$  and pH in acidic efflorescent clay ( $p < 0.01$ ).

with an average of  $7.86 \mu\text{g}\cdot\text{g}^{-1}$ . Therefore, the samples contained ionic fluorine compounds such as KF or NaF.

#### Presence of Acid in Clay

As mentioned above, 60% of the clay samples in this study showed significant acidity ( $\text{pH} \leq 5.6$ ), which indicated that there was a considerable amount of acid dissolved in water. In order to explore the specific form of acid in clay, acidic clay was chosen and the  $p(\text{SO}_4^{2-})$  value was calculated based on its sulfate content ( $\mu\text{g}\cdot\text{g}^{-1}$ ) (Table 1). There was a significant positive correlation between pH and  $p(\text{SO}_4^{2-})$ , according to chemical equilibrium ( $R = 0.75$ , Fig. 3). Here,  $p(\text{SO}_4^{2-})$  is the negative logarithm of sulfate content in the condensate (i.e.,  $-\log C(\text{SO}_4^{2-})$ ), and  $C(\text{SO}_4^{2-})$  was calculated from the sulfate content  $m(\text{SO}_4^{2-})$  in Table 1 and given in  $\text{mol}\cdot\text{L}^{-1}$  in line with the volumetric method. The results

indicated that the acidic substance in clay samples may contain acidic sulfates (probably  $\text{NaHSO}_4$  or  $\text{KHSO}_4$ ), similar to the acidic buffer system  $\text{HSO}_4^- \text{SO}_4^{2-} \cdot n\text{H}_2\text{O}$ , which may have maintained the persistent presence of acid (i.e.,  $\text{H}^+$ ) in clay to some extent. This result is consistent with the results of previous studies on the acidic characteristics of surface soil in Hehua Village, Zhijin, Guizhou [36].

#### Weathering of Clay-Pyrite in Clay

The representative positive and negative ion mass spectra obtained in the high mass resolution mode are shown in Figs 4 and 5, respectively. The detected ions were rich and complex, the cause of which was probably the mixing of the pyrite and clay in the analysis area. The clay was also rich in organic matter. The chemical composition corresponding to each peak was determined by combining the precise mass at a sufficient mass resolution and an isotopic peak. For example, the S and Fe peaks (Figs 4 and 5, respectively) were visible under partial amplification. Interference from organic matter was easily eliminated using the concept of mass loss. After precise mass retrieval and isotopic ratio testing, the most abundant inorganic ions were mainly Fe, S, Al, Si, and O.

The ion images of the clay samples are shown in Figs 6 and 7. The shading in these images correlates with the ion counts and depicts the concentration distribution pattern of specific ion species in a  $400 \mu\text{m} \times 400 \mu\text{m}$  microdomain. Bright bands, such as those from left to right in the S<sup>-</sup> images, indicate areas of highly concentrated sulfur. Dark bands such as those of Si<sup>+</sup> in the same region as above indicate a lack of clay. Ion imaging data indicated that pyrite ( $\text{FeS}_2$ ) was present in the samples. The distributions of the characteristic ions  $\text{FeS}^+$ ,  $\text{FeS}_2^+$ , and S<sup>-</sup> were consistent (Fig. 6, top). Clay minerals were also abundant in the study area. The distributions of the characteristic ions

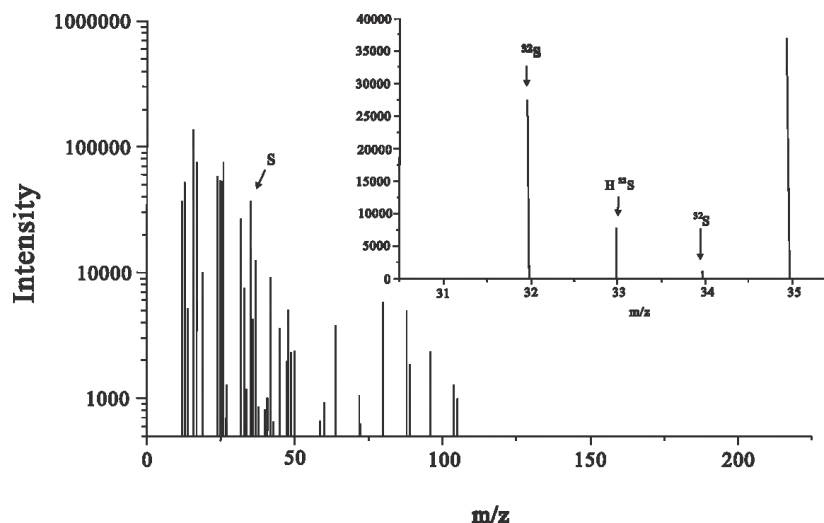


Fig. 4. Negative ion mass spectrum of the clay-pyrite sample.

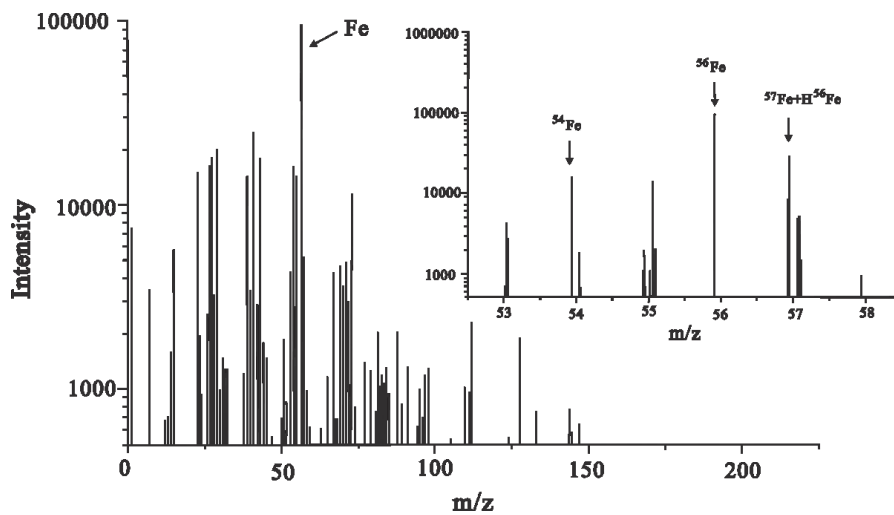


Fig. 5. Positive ion mass spectrum of the clay-pyrite sample.

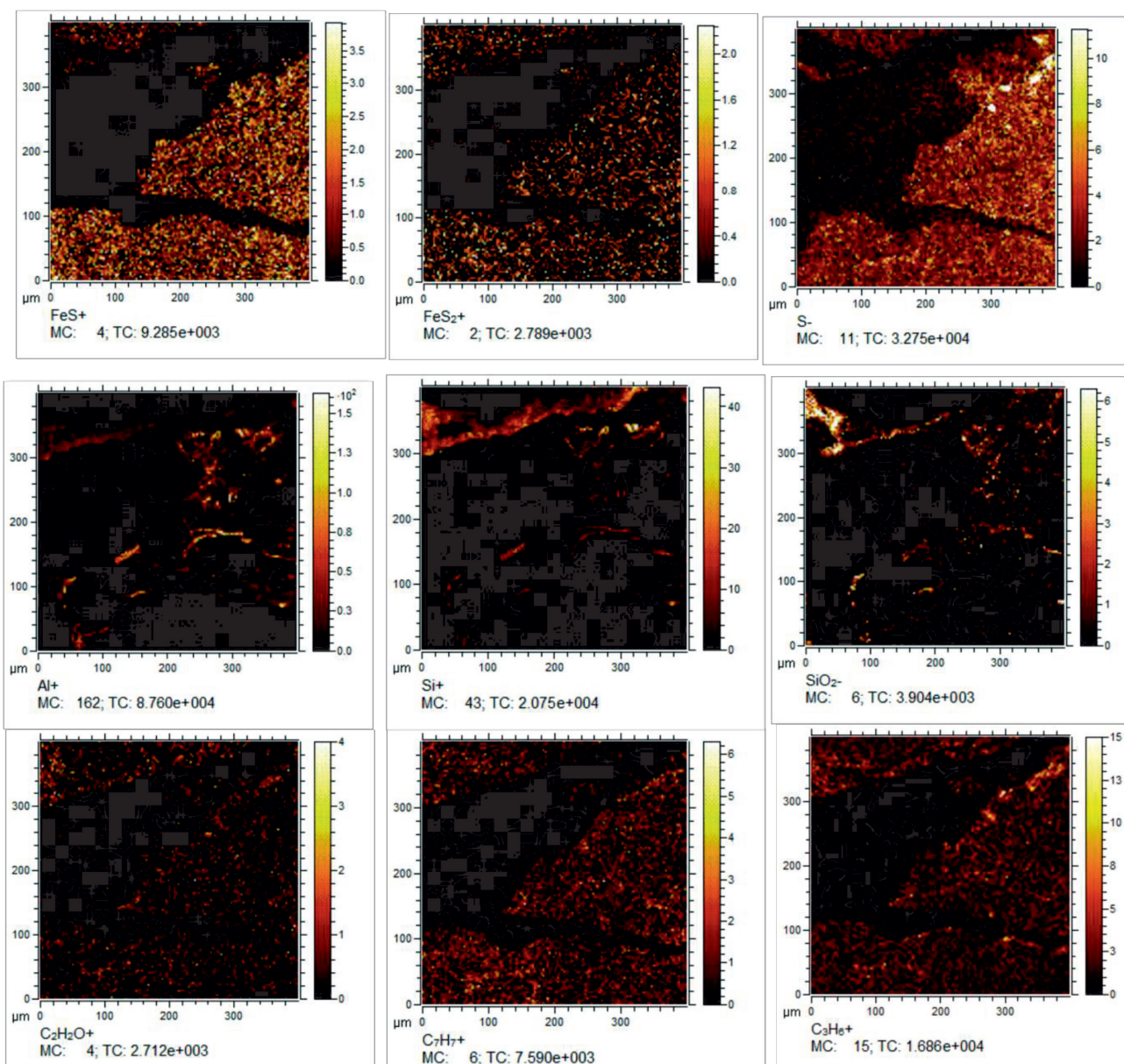


Fig. 6. Typical ion imaging spectrum of clay-pyrite.

Al<sup>+</sup>, Si<sup>+</sup>, and SiO<sub>2</sub><sup>-</sup> (Fig. 6, middle) were also consistent. The distributions of clay minerals and pyrite were complementary. Finally, the organic matter, which made up the least mass in the samples, had the characteristic ions C<sub>7</sub>H<sub>7</sub><sup>+</sup>, C<sub>2</sub>H<sub>2</sub>O<sup>+</sup>, and C<sub>3</sub>H<sub>6</sub><sup>+</sup> (Fig. 7, bottom). The distributions of organic matter in both pyrite and clay minerals were clear. This reflects the enrichment of organic matter in the natural clay-pyrite sample.

The ion imaging data further indicated that the typical ion composition of weathered clay-pyrite was HSO<sub>4</sub><sup>-</sup>, SO<sub>4</sub><sup>-</sup>, and SO<sub>3</sub><sup>-</sup> (Fig. 6, top), which were distributed similarly to that of pyrite (Fig. 6, top). This is indicative of the close relationship between the two, with the characteristic ions of the former likely to be the products of the latter's weathering (oxidation). These characteristic ions were previously detected in the

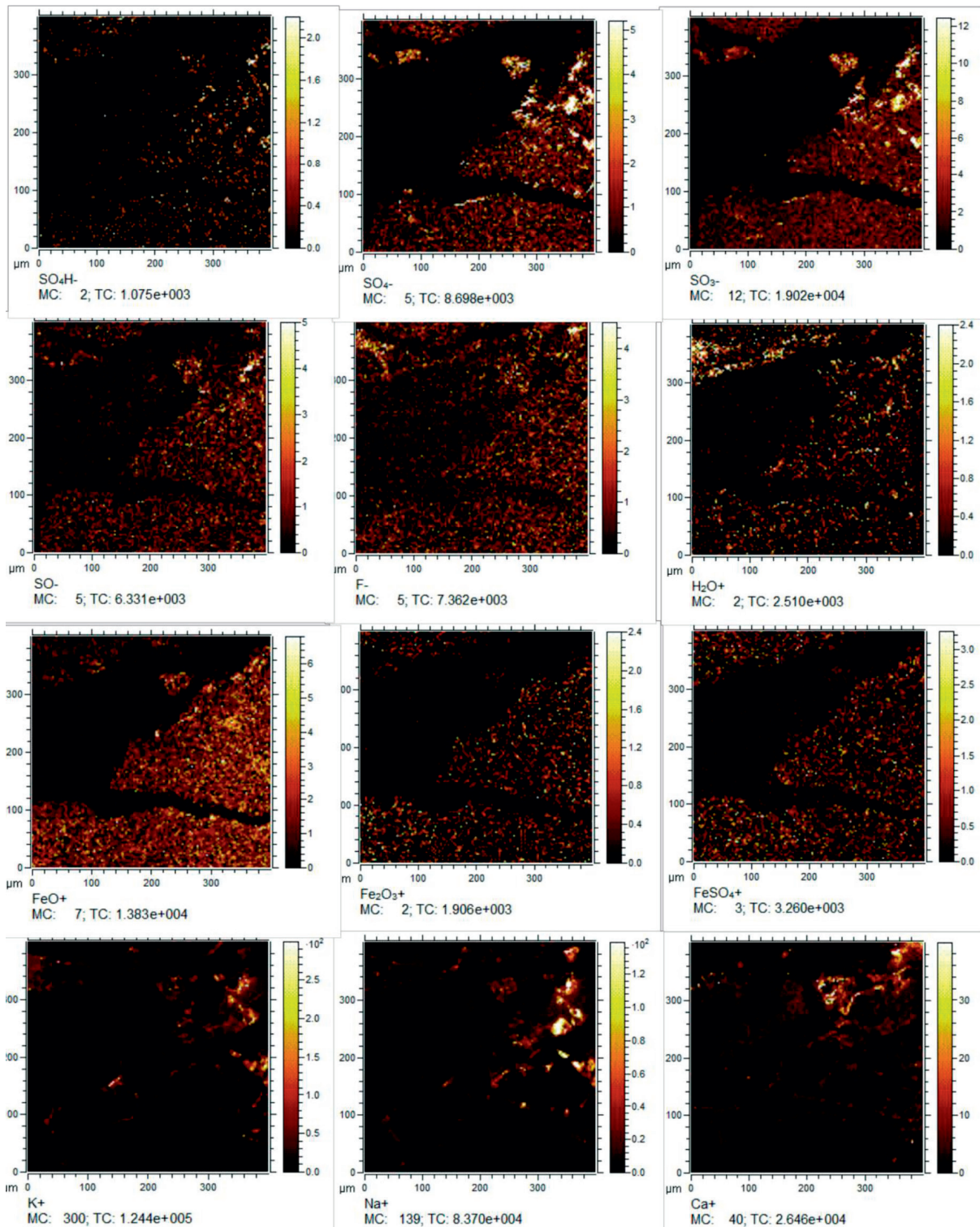


Fig. 7. Characteristic ion imaging spectrum of clay-pyrite weathering.

naturally outcropping coal of northwest Guizhou [15]. After combining this finding with the results of on-site coal combustion tests, the TOF-SIMS characteristic peak was deemed to be either that of sulfuric acid or hydrogen sulfate. Specifically,  $\text{HSO}_4^-$  could have been derived from  $\text{H}_2\text{SO}_4$  molecules,  $\text{HSO}_4^-$  and  $\text{SO}_4^-$ , while  $\text{SO}_3^-$  was a reasonable fragment ion (minor SIMS peak) of the former. The Fe ions include  $\text{FeO}$ ,  $\text{Fe}_2\text{O}_3^+$ , and  $\text{FeSO}_4$  (Fig. 7, middle). Their distributions were similar to that of pyrite (Fig. 6, top) but differed from that of the clay minerals (Fig. 6, middle). This further indicated that the pyrite in the sample underwent a certain degree of weathering (oxidation).

The ion images show that  $\text{F}^-$ ,  $\text{Ca}^+$ , and  $\text{K}^+$  were present in the samples (Fig. 7, middle and bottom). The signal of  $\text{F}^-$  is strong, reflecting the fact that the fluorine content in the clay is high. There is a partial overlap between the  $\text{Ca}^+$  and  $\text{F}^-$  distribution images, suggesting that there is a likelihood of fluorine-containing stable minerals with some covalent bond characteristics, such as fluorite, being present in the samples. Fluorine is partially present in the sample clay as an easily ionizable ionic compound, whereas ionic compounds, such as sodium fluoride ( $\text{NaF}$ ) and potassium fluoride ( $\text{KF}$ ), are readily soluble in water. At the same time, the detected  $\text{Na}^+$  and  $\text{K}^+$  partially agree with the  $\text{F}^-$  image, which also supports the presence of fluorine in the clay samples as ionic fluoride compounds.

Although the patterns from ion imaging mass spectrometry analysis of the different microdomains in the 20 clay samples differed greatly, pyrite ( $\text{FeS}_2^+$ ), the products of pyrite weathering (such as  $\text{HSO}_4^-$ , Fe ions including  $\text{FeO}$ ,  $\text{Fe}_2\text{O}_3^+$ , and  $\text{FeSO}_4$ ), and  $\text{F}^-$  were detected in all the microdomains of each sample, indicating that both pyrite and acid sulfate were found in the clay samples from the villages investigated, which directly points out that the acid in the clay originated from pyrite weathering.

### Release of Hydrogen Fluoride

To investigate the release of hydrogen fluoride from clay under relatively mild conditions, backup clay samples (2.0 g) were heated to approximately  $400^\circ\text{C}$  in a digital thermal control electric jacket (SKM, Heze, China). The headspace gas was analyzed using a G1105 HF analyzer (Picarro, USA) to determine the HF concentration. The HF concentrations of the headspace gas are listed in Table 1. The HF concentrations were in the range of 28–302 ppb, with an average of 105.67 ppb, which was higher than the HF background concentration in the laboratory. These results showed that heating of the clay samples led to HF release without exception, providing direct evidence of HF release during the heating process. The significant differences among the HF concentrations for the different coal samples might be due to variations in the fluorine content, pH, or degree of heating. There was a positive correlation between HF concentration and coal pH ( $R = 0.78$ ,

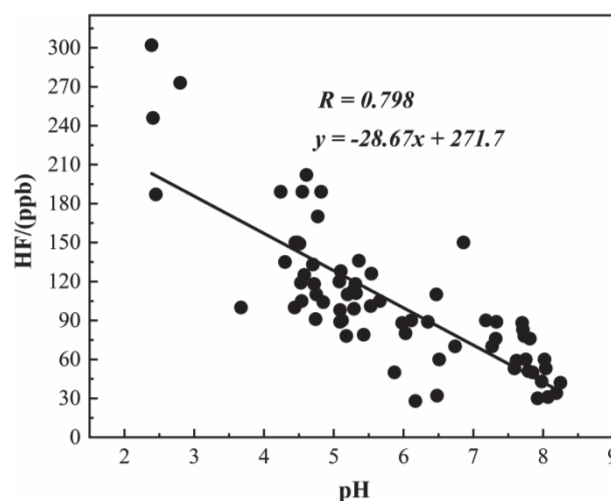


Fig. 8. Correlation between pH and HF in clay.

Fig. 8), indicating that higher clay acidities caused more HF to be released. Therefore, it was concluded that the acid in the coal contributed to the HF release.

### Discussion

The coal-bearing strata of the Late Permian Longtan Formation occur extensively in northwest Guizhou as well as in the adjacent provinces of Yunnan and (localized areas of) Sichuan. Mountains and ravines were formed during tectonic movements in the geological past. At the same time, there was extensive outcropping of coal-bearing strata [16, 41, 42], including alternating coal seams and clay layers within the Longtan Formation. This research confirmed that, similar to coal, clay is also generally acid-rich and contains sulfates [31]. For example, the clay prototype, corresponding to the sample used in this study (DF2T-1), was acidic ( $\text{pH} = 2.45$ ) and contained as much as  $12,865 \mu\text{g}\cdot\text{g}^{-1}$  of sulfate ( $\text{SO}_4^{2-}$ ). The amount of fluorine and natural water contained in the proto-sample was also high ( $1,764 \mu\text{g}\cdot\text{g}^{-1}$  and 37%, respectively) [29].

This study verified that the acidification of the clay in the coal-bearing strata was likely caused by the natural weathering of pyrite ( $\text{FeS}_2$ ) under long-term exposure to atmospheric oxidizing processes. The residual acids or sulfates ( $\text{HSO}_4^-$ ) from this weathering reaction were retained in the strata. Unfortunately, this type of clay is also generally high in fluorine. As shown in Table 1, the total fluorine content of the clay was  $237\text{--}1,764 \mu\text{g}\cdot\text{g}^{-1}$ , with ionic fluoride ranging from  $1.47$  to  $20.61 \mu\text{g}\cdot\text{g}^{-1}$ . Given the inherent nature of clay as an aqueous gel, it is often used as a binder for mixing with locally crushed or pulverized coal to become a fuel for burning in daily living [4]. During the combustion process, the retained sulfates and fluorine are likely to follow reaction formula (1) below. Hydrogen fluoride is produced in gaseous and aerosol forms, releasing fluorine into the atmosphere.

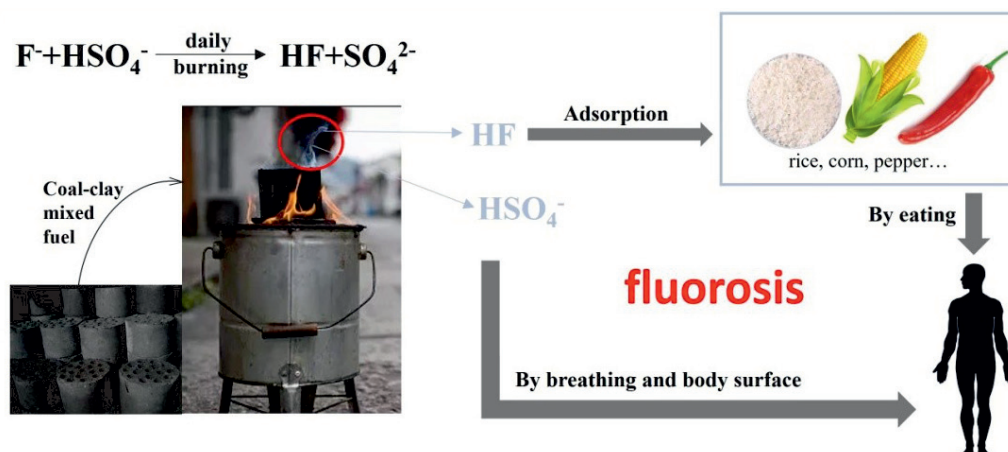
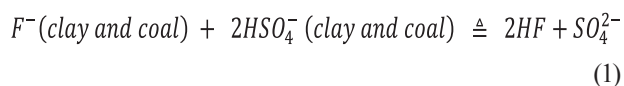


Fig. 9. Schematic diagram of source and pathways of endemic fluorosis in Southwest China.

This exacerbates fluorine pollution in the rooms of local rural dwellings, resulting in human exposure and health issues (Fig. 9).



The role of clay in coal-burning fluorosis has also been emphasized in previous studies by other scholars. Dai et al. [20], Wu et al. [19], Luo et al. [15], Li et al. [40], Li et al. [43] and Hong et al. [29] all pointed out that the clay for coal burning is an important source of fluoride emission from coal burning. However, previous studies mainly analyzed the fluorine content in clay to judge its influence on endemic fluorosis. This study not only analyzed the physical and chemical properties of the clay samples, such as acidity, fluorine content and sulfate content, but also analyzed the occurrence form of acid in clays at micro level by TOF-SIMS, and further discussed the release mechanism of fluorine and the catalytic effect of acid on fluorine release from clays. In addition, the release form of fluorine (HF) from clays was confirmed by heating experiment. According to our previous survey, the temperature of the open furnace was between 300 and 400°C in the endemic fluorosis area of Guizhou. When heating and cooking are not required, the furnace is closed and its temperature is generally below 200°C. At this temperature, fluorine in the coal would first be released in the form of HF, instead of KF or NaF. As the boiling point of HF is only 19.5°C, while the boiling points of NaF, KF, and CaF<sub>2</sub> are 1695, 1505, and 2500°C, respectively. This study had provided new evidence to further explain the cause and mechanism behind the once-endemic fluorosis in the local area, which results from the coupling of natural and human activities. Previous studies showed that heating of outcrop coal also released HF [8], and further studies were conducted to determine the contribution of fluorine released from clay during coal burning and the fluorine species during transfer among the coal,

food and the human body. For example, it is unknown if fluoride is the only form of fluorine in smoke dust aerosol, or if the digestive system is the sole pathway for human intake of fluorine in endemic fluorosis. The occurrence of these forms needs to be further verified.

## Conclusion

In this study, TOF-SIMS was used to analyze a typical clay-pyrite sample, which revealed that the clay-pyrite in the naturally outcropping coal series in northwest Guizhou had undergone weathering, with HSO<sub>4</sub><sup>-</sup> and sulfates (SO<sub>4</sub><sup>2-</sup>) being the residual products from these oxidization reactions, which promote the release of fluoride in the form of HF from the clays. This provided further understanding of the mechanism of the coupling of natural and human activities of endemic fluorosis in the local area. The pH of 71 clay samples from this area ranges from 2.39 to 8.25 with an average of 5.81. The coal samples also exhibits high level of sulfate content, ranging from 295 to 13086 μg.g<sup>-1</sup>, with an average of 1851 μg.g<sup>-1</sup>, and the fluorine concentration ranged from 237 to 1764 μg.g<sup>-1</sup> (average 751 μg.g<sup>-1</sup>). The positive relationship between pH and *p*(SO<sub>4</sub><sup>2-</sup>) of the acidic clay suggested that the acid might be in the form of acidic sulfate HSO<sub>4</sub><sup>-</sup>. Further research using TOF-SIMS confirmed the presence of HSO<sub>4</sub><sup>-</sup>. The heating experiment verified that HF was released from coal without exception, and a positive correlation was found between HF concentration and clay pH. The possible reaction mechanism is that the prevalence and coexistence of the acid (HSO<sub>4</sub><sup>-</sup>) and fluorine lead to a reaction producing hydrogen fluoride (HF) under combustion and mild heating. This finding may change current understanding of the cause and prevailing mechanism of coal-burning endemic fluorosis. In the follow-up study, the mechanism of coal-burning fluorosis was further analyzed and further studies should be conducted to determine the contribution of fluorine released from clay during coal burning and

the fluorine species during transfer among the coal, food and the human body.

### Acknowledgment

This work was supported by the Anhui Natural Science Foundation Project (No. 2008085QD169), National Natural Science Foundation of China (No. 41902172 and 41772157), and Natural Science Research Project of Colleges and Universities in Anhui Province (No. KJ2020A1204). We would like to give special thanks to Jing Lei, Shan Li, Yao Li, and Daiyi Wang for their support with sampling.

### Conflict of Interest

The authors declare that we have no financial and personal relationships with other people or organizations that can inappropriately influence our work.

### Reference

- LYTH O. Endemic fluorosis in Kweichow, China. *The Lancet*, **1**, 233, **1946**.
- PH H., LUO K., ZHANG S. Risk assessment model for different foodstuff drying methods via AHP-FCE method: A case study of “coal-burning” fluorosis area of Yunan and Guizhou Province, China. *Food Chem.*, **263**, 74, **2018**.
- WANG X.L., MING J., QIU B., Relationship between fluoride exposure, orthopedic injuries and bone formation markers in patients with coal-burning fluorosis. *Chin J of Appl Ecol.*, **30**, 43, **2019**.
- HE L.L., HE S.Y., CHEN Z.Y., Fluorine Pollution in the Environment and Human Fluoride Effect. *Earth Environ.*, **48**, 87, **2020**.
- KASHYAP S.J., SANKANNAVAR R., MADHU G.M., Fluoride Sources, Toxicity and Fluorosis Management Techniques - A Brief Review. *Journal of Hazard Materials Letters*, **2**, 100033 **2021**.
- LUO K.L., LI L., ZHANG S.X., Coal-burning roasted corn and chili as the cause of dental fluorosis for children in southwestern China. *J Hazard Mater.*, **185**, 1340, **2011**.
- LIU Y.L., LUO K.L., LI L., Fluoride and sulphur dioxide indoor pollution situation and control in coal-burning endemic area in Zhaotong, Yunnan, China. *Atmos Environ.*, **77**, 725, **2013**.
- HONG X.P., LIANG H.D., ZHANG Y. Evaluation of acidity in late Permian outcrop coals and its association with endemic fluorosis in the border area of Yunnan, Guizhou, and Sichuan in China. *Environ Geochem Hlth.*, **40**, 1093, **2018**.
- XIONG Y., NING Z.P., LIU Y.Z., XIAO T.F., Geochemical behavior of fluorine and molybdenum in coals and soils in coal-burning related endemic area in southwest China. *Earth Environ.*, **49**, 1, **2021**.
- YU Y.Q., ZHANG X.X., TIAN W., LI F.C., WU C.X., ZHANG T., GUAN Z.Z., Analysis of Dental Fluorosis and BMI of Adults in Coal-burning Endemic Fluorosis Areas in Western Guizhou Province. *J Guizhou Med Univ.*, **40**, 7, **2020**.
- GIBERGANS-BÁGUENA J., JARAUTA-BRAGULAT E. The Quality of Urban Air in Barcelona: A New Approach Applying Compositional Data Analysis Methods. *Emerg Sci J.*, **4**, 113, **2020**.
- ZHENG B.S., DING Z.H., HUANG R.G., ZHU J.M., Yu X.Y., WANG A.M., Issues of health and disease relating to coal use in southwestern China. *Int J Coal Geol.*, **40**, 119, **1999**.
- LI R.B., TAN J.N., WANG W.Y., Discussion on fluorosis source for endemic fluorosis caused by food in Guizhou. *Nati Med J China.*, **62**, 425, **1982**.
- FIKKNMAN R.B., Potential health impacts of burning coal beds and waste banks. *Int J Coal Geol.*, **59**, 19, **2004**.
- LUO K.L., LI H.J., FENG F.J., CHEN T.B., XIONG M.H., WANG W.Z., LIAO X.Y., Li W., WANG L.H., Content and distribution of fluorine in rock, clay and water in fluorosis area Zhaotong, Yunnan Province. *J China Coal Soc*, **32**, 363, **2007**.
- LUO K.L., LI L., ZHANG S.X. Coal-burning roasted corn and chili as the cause of dental fluorosis for children in southwestern China. *J Hazard Mater*, **185**, 1340, **2011**.
- ZHOU D.X., FU Q., Fluorosis mode of little white mouse caused by baked food by coal with different fluorine content. *Nati Med J China*, **65**, 692, **1985**.
- ZHOU D.X., FU Q., WANG Z.L., ZHOU, C. Investigations on the relationship between the fluorine content in the clay mixed with coal and the endemic fluorosis caused by coal-burning. *Chin J Control of Endemic Dis*, **6**, 243, **1991**.
- WU D.S., WANG A.M., ZHENG B.S., WANG, D.D., Investigation of the prevalent status on coal-burning pollution endemic fluorosis in some areas in northwestern Guizhou. *Chin J Endemiol*, **23**, 454, **2004**.
- DAI S.F., LI W.W., TANG Y.G., ZHANG Y., FENG P. The sources, pathway, and preventive measures for fluorosis in Zhijin County, Guizhou, China. *Appl Geochem*, **22**, 1017, **2007**.
- CHEN G.W., TIAN J.C., QIN, Y., Study on the sources of endemic fluorosis in Weixin, Yunnan Province, China. *Int J Min Sci Technol*, **36**, 241, **2007**.
- XIE X.N., YANG X.Z., YANG S.Y., ZHANG J.J., ZHAO B., A tentative discussion on the source of endemic fluorosis: Geo-environmental evidence from three counties in Guizhou Province. *Geol China*, **37**, 696, **2010**.
- LIU X.F., LIU C.G., LIU J., ZHANG J.Y., SONG D.Y. Analysis on fluorine speciation in coals from Guizhou Province. *Proceedings of the CSEE.*, **28**, 46, **2008**.
- HONG X.P., LIANG H.D., LV S. Release of hydrogen fluoride from clay used for coal-combustion in Zhijin county, Guizhou province, Peoples' Republic of China. *Fluoride.*, **50**, 182, **2017**.
- LI M., QU X., MIAO H., WEN S., HUA Z., MA Z., HE Z. Spatial distribution of endemic fluorosis caused by drinking water in a high-fluorine area in Ningxia, China. *Environ. Sci. Pollut. Res.*, **27**, 20281, **2020**.
- HE L.L. Study on the distribution characteristics of fluorine in different geological background areas and the levels of human fluoride exposure. *Guiyang: Guizhou University*, **2020**.
- LIANG H.D., GARDELLA J.A.J., HE P., YATZOR B.P. Potential release of hydrogen fluoride from domestic coal in endemic fluorosis area in Guizhou, China. *Chin Sci Bull.*, **56**, 2301, **2011**.
- AAAS news. [http://esciencenews.com/sources/physorg/2011/10/01/hydrogen fluoride may be major cause coal burning endemic fluorosis](http://esciencenews.com/sources/physorg/2011/10/01/hydrogen%20fluoride%20may%20be%20major%20cause%20of%20coal%20burning%20endemic%20fluorosis).

29. HONG X.P., LIANG H.D., ZHANG Y.F., XU D.M. Acidity characteristic of efflorescent clay in late Permian coal-bearing strata in border area of Yunnan, Guizhou and Sichuan. *Environ Chem.*, **36**, 1831, **2017**.
30. HONG X.P., LIANG H.D., ZHANG Y. Evaluation of acidity in late Permian outcrop coals and its association with endemic fluorosis in the border area of Yunnan, Guizhou, and Sichuan in China. *Environ Geochem Health.*, **40**, 1093, **2018**.
31. HONG X.P., LIANG H.D., ZHANG Y.F., XU D.M. Distribution of acidity of late Permian coal in border area of Yunnan, Guizhou, and Sichuan. *J China Coal Soc.*, **41**, 964, **2016**.
32. XIONG Y., XIAO T., LIU Y., ZHU J., NING Z., XIAO Q. Occurrence and mobility of toxic elements in coals from endemic fluorosis areas in the three gorges region, sw china. *Ecotox & Environ Safe.*, **144**, 1, **2017**.
33. CAO Q.Y., LIANG H.D., YANG L. Analysis of mercury speciations in Late Permian coal from the border area of Yunnan, Guizhou and Sichuan province. *China Environ Sci.*, **39**, 3959, **2019**.
34. LIU Y.H., HONG X.P., LIANG H.D., LI Z.P. Weathering of coal-series clay-pyrite in the area of desulfurization in Guizhou Province. *Environ Chem.*, **38**, 1318, **2019**.
35. LIU J., YANG S., LUO M.J., ZHAO X., ZHANG Y.M., LUO Y. Association of dietary carotenoids intake with skeletal fluorosis in the coal-burning fluorosis area of guizhou province. *Biomed Environ Sci.*, **31**, 438, **2018**.
36. HONG X.P., LIANG H.D., LV S., WANG D.Y., ZHANG Y., Potential Release of Fluoride from Clay for Coal-Combustion in Hehua Village, Zhijin County, Guizhou Province. *Geol Rev.*, **4**, 852, **2015**.
37. SHI Z.J., ZHANG J.E., XIAO Z.H., LU T.T., REN X.Q., WEI H. Effects of acid rain on plant growth: a meta-analysis. *J Environ Manage.*, **297**, 113213, **2021**.
38. ZHENG Y.C., LIAO L.P., LIU Y. Investigation on the background fluorine content of soil in Guizhou and its relationship with fluorosis. *Stud Trace Elem Health.*, **26**, 39, **2009**.
39. PAN Z.P., LIU X.H., MENG W. Geochemical characteristics of fluorine in soils and its environmental quality in central district of Guiyang. *Res Environ Sci.*, **31**, 87, **2018**.
40. LI H.J., LUO K.L., WU X.Z. Effect of clay on coal-combustion fluorine pollution in Zhaotong. *J China Min Technol.*, **37**, 802, **2008**.
41. XU B.B., HE M.D. Coal geology of Guizhou. Xuzhou: China University of Mining and Technology Press., **5**, **2002**.
42. LIU W.D., LI J.J., GUO X.G. Analysis of fluoride pollution situation and source in poor rural areas of Guizhou Province. *Earth Environ.*, **41**, 138, **2013**.
43. LI L., LUO K.L., TANG Y.G., Mechanism of fluorine releasing in coal and clay and its effects on environment in Zhaotong, Yunnan Province. *Chin J Endemiol.*, **34**, 34 (8), 569, **2015**.